

Article

Early Age Sealing Capacity of Structural Mortar with Integral Crystalline Waterproofing Admixture

Calin Mircea ^{1,*}, Tudor-Panfil Toader ^{1,2}, Andreea Hegyi ², Brăduț-Alexandru Ionescu ^{1,2} and Andreea Mircea ¹ 

¹ Civil Engineering Faculty, Technical University of Cluj-Napoca, 28 Memorandumului Street, 400114 Cluj-Napoca, Romania; tudor.toader@incerc-cluj.ro (T.-P.T.); bradut.ionescu@incerc-cluj.ro (B.-A.I.); andreea.mircea@ccm.utcluj.ro (A.M.)

² NIRD URBAN-INCERC Cluj-Napoca Branch, 117 Calea Floressti, 400524 Cluj-Napoca, Romania; andreea.hegyi@incerc-cluj.ro

* Correspondence: calin.mircea@dst.utcluj.ro; Tel.: +40-(0)-728-555980

Abstract: Crystalline admixtures embedded in concrete may react in the presence of water and generate thin crystals able to fill pores, capillaries and micro-cracks. Once the concrete has dried, the crystalline chemicals sit dormant until another dose of water starts the crystallization again. The research aims to analyse the early age self-sealing effect of a crystalline admixture at a dosage rate of 1–3% of the cement mass. Specimens made with two types of gravel were pre-loaded with three-point bending to up to 90% of the ultimate capacity, and conditioned through wet–dry cycles. Micro-crack closure was measured with a microscope after pre-loading, and after 1 day, 4 days, 8 days, 14 days and 20 days of wet–dry exposure. The results show that an admixture content of 3% achieves the best early self-sealing performance. These results are also confirmed by probabilistic analyses, which also emphasize the self-sealing potential of lower ICW contents.

Keywords: mortar; self-sealing; micro-cracks; crystalline admixtures; early age; grain size; probabilistic analysis



Citation: Mircea, C.; Toader, T.-P.; Hegyi, A.; Ionescu, B.-A.; Mircea, A. Early Age Sealing Capacity of Structural Mortar with Integral Crystalline Waterproofing Admixture. *Materials* **2021**, *14*, 4951. <https://doi.org/10.3390/ma14174951>

Academic Editor: Eddie Koenders

Received: 7 August 2021

Accepted: 27 August 2021

Published: 30 August 2021

Publisher's Note: MDPI stays neutral with regard to jurisdictional claims in published maps and institutional affiliations.



Copyright: © 2021 by the authors. Licensee MDPI, Basel, Switzerland. This article is an open access article distributed under the terms and conditions of the Creative Commons Attribution (CC BY) license (<https://creativecommons.org/licenses/by/4.0/>).

1. Introduction

Cementitious composites have been widely used all over the world since the spectacular development of Portland Cement in the 19th century. Even in traditional/initial forms (e.g., ordinary concrete), cementitious composites have proven their remarkable autogenous self-healing ability, as became well known in the same period [1,2], attributed at that time to the ongoing hydration reaction. However, the phenomenon was neglected for many decades, and it was not until the end of the 19th century when researchers' interest was piqued by this self-sealing potential and its ability to reduce early age cracking [3–5]. More recently, the contribution of tensile creep was also considered for restrained shrinkage, and significant research has been initiated on the topic to quantify the creep tensile strain [6–8].

Self-healing can potentially have a great impact upon the durability of concrete structures, especially on those exposed to severe conditions. Within the last few decades, significant research has been done to improve the knowledge of the relevant mechanisms, and to develop new concepts and techniques [9–16]. We can now identify three major self-healing processes/techniques: autogenous self-healing, encapsulated autonomous self-healing and self-healing bio-concrete. Given the nature of the present work, only autogenous self-healing will be discussed in this paper.

Cementitious materials possess a natural autogenous healing capacity by filling micro-cracks through four mechanisms: the continued hydration of unhydrated cement, calcium carbonate precipitation, the expansion/swelling of calcium-silicate hydrate gel, and the deposition of impurities such as water (e.g., debris and spall crack) [17–20]. The first two mechanisms are the most important. At an early age, continued hydration seems to make

the greatest contribution, while for mature concrete the second mechanism becomes essential [21]. Crack widths of up to 300–400 μm have been reported to be cured by autogenous healing in the presence of water [12,22]. The major factors that influence the process are mix composition, concrete age, water presence and crack shape and width [23,24]. Besides the natural/intrinsic ability, autogenous healing potential can also be stimulated. Mineral additives, such as blast-furnace slag and fly ash, significantly improve autogenous healing when used to partially replace Portland cement [18,25–30] through ongoing hydration. Limestone powder, marble slurry and hydrated lime increase the calcium content and act as a site for the nucleation of cement hydration [31–34], being sustainable replacements for cement [35]. Superabsorbent polymers induce self-healing by providing an ongoing reservoir of water for hydration. By encouraging multiple cracking, more narrow cracks occur [36]. These also stimulate further hydration [37,38].

Integral crystalline waterproofing (ICW) admixtures embedded in concrete contain crystalline chemicals that react in the presence of water and generate thin crystals able to fill pores, capillaries and micro-cracks [39]. As long as moisture remains present, crystals continue to grow inside concrete. Once the concrete has dried, the crystalline chemicals sit dormant until another dose of water, e.g., supplied through a new crack, causes the chemical reaction, known as crystallization, to start again [40–45]. Mortars with crystalline and expansive additives have also been proven to have higher pH values, which favor calcium carbonate precipitation [22].

The research provides experimental evidence of the early self-sealing potential of ICW admixtures. A powder ICW admixture was added in percentages of 1–3% of the mass of the Portland cement, based on the producer’s recommendations.

The ICW’s self-sealing potential was assessed on two types of mortar mixes. The first used typical quartz sand with a maximum grain size of 2 mm, in accordance with EN 933-1:2012. The second considered a quartz gravel of up to 4 mm, in an attempt to study the self-sealing potential of the local available gravel in mixes with higher porosity and diversified fracture behavior [46–48].

In summary, the main objective of this research was to analyze the early self-sealing potential of mortars with ICW admixtures with a content of 1–3% of the cement mass. A secondary objective was to determine the changes caused by doubling the maximum grain size of the quartz gravel, from 2 mm to 4 mm, giving rise to fracture processes with diverse parameters. The analyses were performed based on tests, wet–dry conditioning, and analyses of self-sealing parameters from a probabilistic perspective.

2. Materials and Methods

2.1. Ingredients and Mix Proportions

The ingredients and proportions were chosen, starting with the reference mix T0r shown in Table 1, which demonstrated a significant self-healing ability in a previous work [49]. For comparison, the same T0c mix was made with quartz gravel instead of standard quartz sand. Both aggregates had a similar chemical composition, with quartz crystals (i.e., SiO_2) present at more than 96%. Comparative particle size distributions are shown in Figure 1.

Table 1. Reference mix contents T0r and T0c.

Mixture	Cement (kg)	Fly Ash (kg)	Sand/Gravel (kg)	MS (kg)	HRWRA (kg)	Water (kg)	PVA (kg)
T0r	580	650	476	141	12.75	327	26
T0c	580	650	476	141	12.75	327	26

Note: Cement (density: 1.07 g/cm^3), fly ash (density: 0.89 g/cm^3), standard sand (density: 1.65 g/cm^3), fine gravel (density: 1.55 g/cm^3), MS (density: 1.19 g/cm^3), HRWRA (density: 0.77 g/cm^3), water (density: 0.99 g/cm^3), PVA (density: 1.30 g/cm^3). Values were determined with a standard deviation of $\pm 1\%$.

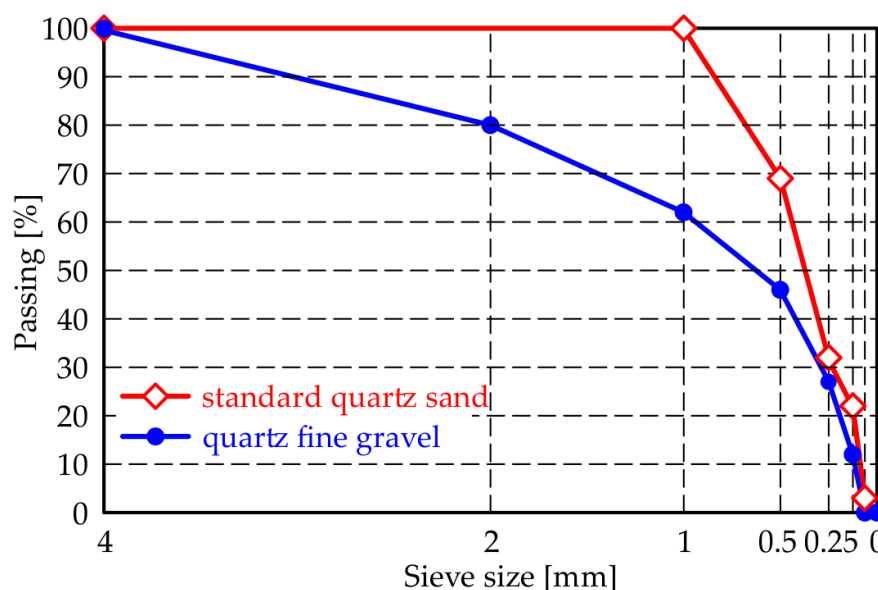


Figure 1. Particle size distribution of the sand and gravel employed in the tested specimens.

A type-C fly ash was added to the Portland cement type CEM I 42.5R, referenced by EN 197-1, in a mass proportion of 1.12. Marble slurry (MS), an important by-product of marble manufacturing, was introduced as a fine aggregate with a size ranging from 75 μm to 4.75 mm. A polycarboxylate-based high-range water-reducing admixture (HRWRA) and synthetic polyvinyl alcohol (PVA) fibers were added to promote the precipitation of crystallization products on the crack’s surface [50,51]. The PVA fibers, with a density of 1300 kg/m^3 , were 8 mm in length and 39 μm in diameter, with a tensile strength of 1.2 GPa and a 1.2% mineral oil coating to reduce the interfacial chemical bond with the matrix. A constant volume fraction of 2% was introduced.

The addition of the ICW powder, with a density of 1.0 g/cm^3 , into the studied mixes was carried out by reducing the C fly ash mass proportion by the same quantity. Figure 2 presents the diffraction pattern of the ICW white powder used. This reveals the high content of hatrurite, trona, calcite, coesite and albite crystals, all with direct impacts upon the self-sealing ability.

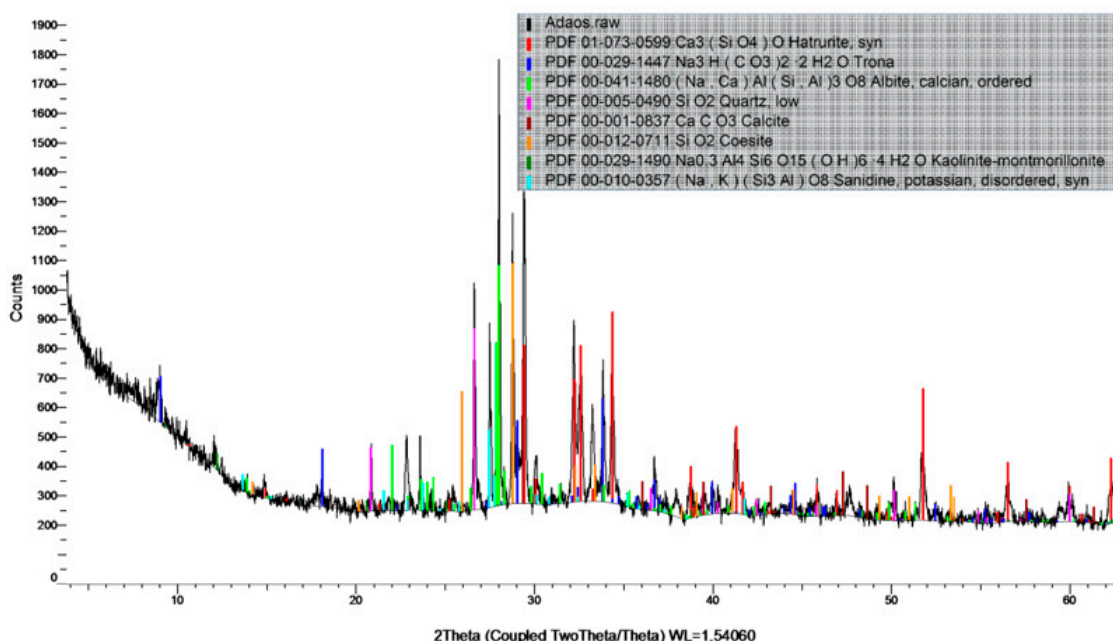


Figure 2. X-ray diffraction result of the ICW powder.

The mix proportions are shown in Table 2 in relative mass proportions.

Table 2. Relative mass mix proportions.

Mixture	Cement	Fly Ash	Sand/Gravel	MS	HRWRA	Water	PVA	ICW
T0r ¹ , T0c ²		1.12						-
T1r ¹ , T1c ²	1	1.11	0.82	0.24	0.02	0.56	0.04	0.01
T2r ¹ , T2c ²		1.10						0.02
T3tr ¹ , T3c ²		1.09						0.03

¹ Specimens made with standard quartz sand; ² Comparative specimens made with quartz gravel.

2.2. Specimen Preparation, Preloading and Conditioning

After mixing, the fresh mortar mixtures were cast into 40 × 40 × 160 mm molds, covered in plastic foil, and stored in a climatic chamber at 20 ± 2 °C and 90% relative humidity (RH). After 24 h, the specimens were removed from the molds and water-cured for 28 days under room conditions (i.e., 20 ± 2 °C and RH = 50%). After that, three specimens of each mixture were subjected to preliminary three-point bending tests (see Figure 3), and another three specimens were cracked by pre-loading up to 90% of the mean flexural strength (i.e., modulus of rupture) previously determined. The results of the preliminary three-point bending tests are given in Table 3. The densities of the hardened mortar samples, determined with the same standard deviation of ±1%, are also shown in Table 3.

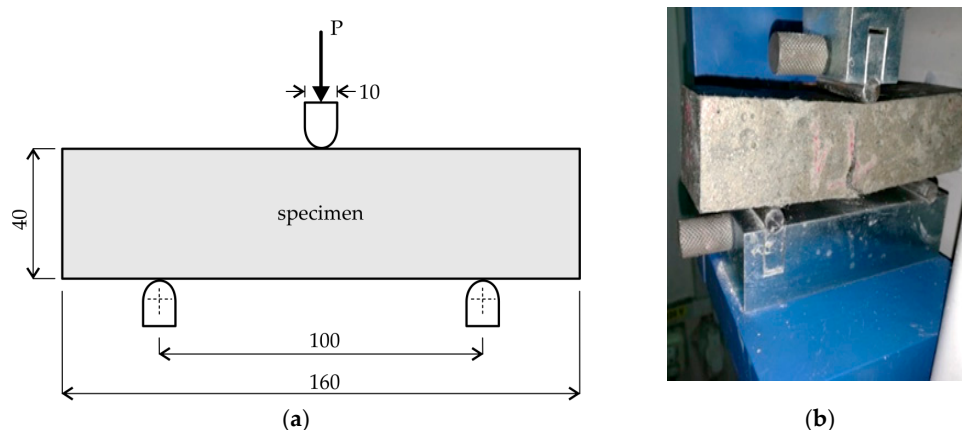


Figure 3. Schematics of the preliminary test set up: (a) EN 196-1 three-point bending (dimensions in mm); (b) specimen under flexural failure.

Table 3. Modulus of rupture for the tested specimens and mixtures.

Mixture	Density (kg/m ³)	Effective Flexural Strength (MPa)	Mean Flexural Strength (MPa)
T0r	1921	17.2/16.7/16.3	16.7
T1r	1923	16.9/15.1/15.2	15.7
T2r	1927	18.2/20.1/18.5	18.9
T3r	1931	19.3/21.5/19.8	20.2
T0c	1918	15.9/16.4/15.0	15.8
T1c	1922	15.3/16.2/17.2	16.2
T2c	1923	16.7/17.3/14.9	16.3
T2c	1925	16.7/16.1/16.7	16.5

In the end, daily wet–dry cycles were applied for 20 days. Every day, 16 h of water immersion was followed by 8 h of dry exposure under the above room conditions (i.e., 20 ± 2 °C and RH = 50%).

2.3. Self-Sealing Parameters and Evaluation

The micro-crack widths were measured with a Leica DMC2900 microscope just after preloading, and after 1 day, 4 days, 8 days, 14 days and 20 days of wet–dry exposure in daily cycles. Readings were made on segments framed in small areas of 1.6 × 1.3 mm with a magnification factor of 8×. The following time-dependent self-sealing parameters are discussed with regard to both the raw segment data and individual cracks:

- Crack closure, considering the relative decrease in the average crack width w_{av} at day t of conditioning, related to the initial moment after preloading

$$\text{Crack closure [\%]} = \frac{w_{av}(0) - w_{av}(t)}{w_{av}(0)} \times 100 \tag{1}$$

- Closure rate of the crack, considering the decrease in the average crack width related to the corresponding interval t in days

$$\text{Closure rate [\mu m/day]} = \frac{w_{av}(0) - w_{av}(t)}{t} \tag{2}$$

The choice of the above parameters is justified by the fact that they offer a global characterization of the phenomena. Similar to in [41,52], the average crack width was determined on crack segments w_{av}^i , and full cracks w_{av} were determined by:

$$w_{av}^i = \frac{A_{cr}^i}{l_{cr}^i} \tag{3}$$

$$w_{av} = \frac{\sum_i A_{cr}^i}{\sum_i l_{cr}^i} \tag{4}$$

where A_{cr}^i is the area of the crack segment i and l_{cr}^i is the midline crack segment.

The parameters were then analyzed and discussed in the context of the Gaussian distribution, implementing the general form of the probability density function—

$$f(x) = \frac{1}{\sigma\sqrt{2\pi}} \exp\left[-\frac{1}{2} \frac{(x - \mu)^2}{\sigma^2}\right] \tag{5}$$

with the variable x (i.e., crack closure and closure rate), μ as the mean value of the variable x , and σ as its standard deviation.

3. Results and Discussion

3.1. Self-Sealing Crack Closure

Table 4 presents the regression of the individual crack widths registered on all specimens, while Figures 4 and 5 summarize graphically the width progress of the mean cracks in all mixtures.

Table 4. Crack progress in the specimens and mean crack widths for mixtures.

Mixture	Crack Widths (mm) in the Conditioning Period					
	0 Days	1 Day	4 Days	8 Days	14 Days	20 Days
T0r	53.9/65.5/60.4	50.2/60.7/56.1	23.2/37.6/31.1	14.2/25.0/20.1	6.8/12.4/9.9	4.4/9.0/7.0
	59.9 ± 5.8	55.7 ± 5.3	30.6 ± 7.2	19.8 ± 5.4	9.7 ± 2.8	6.8 ± 2.3
T1r	37.2/46.3/34.5	32.5/42.6/31.2	29.4/37.8/27.8	9.3/29.2/17.4	4.7/23.0/12.9	3.2/13.4/7.7
	39.3 ± 6.2	35.4 ± 6.2	31.6 ± 5.3	18.6 ± 10.0	13.5 ± 9.2	8.1 ± 5.1
T2r	53.2/59.1/42.0	50.5/58.1/40.9	36.4/50.8/34.2	21.4/38.9/24.9	13.1/33.0/20.1	8.9/28.6/16.9
	51.4 ± 8.7	49.8 ± 8.6	40.5 ± 9.0	28.4 ± 9.3	22.1 ± 10.1	18.1 ± 9.9

Table 4. Cont.

Mixture	Crack Widths (mm) in the Conditioning Period					
	0 Days	1 Day	4 Days	8 Days	14 Days	20 Days
T3r	32.6/39.0/33.5 35.0 ± 3.5	13.6/32.3/22.0 22.6 ± 9.4	4.3/18.3/11.0 11.2 ± 7.0	1.3/5.6/3.3 3.4 ± 2.1	0.5/1.4/0.9 0.9 ± 0.4	0.2/0.3/0.2 0.3 ± 0.1
T0c	49.3/61.5/61.7 57.5 ± 7.1	41.9/53.6/ 53.2 49.6 ± 6.6	13.2/34.4/27.0 24.9 ± 10.8	8.0/29.6/21.4 19.7 ± 10.9	5.7/25.4/17.7 16.3 ± 9.9	4.6/17.8/10.8 11.0 ± 6.6
T1c	73.5/88.2/76.9 79.5 ± 7.7	72.6/87.2/75.7 78.5 ± 7.7	27.2/46.1/31.9 35.1 ± 9.8	10.2/28.4/12.9 17.3 ± 10.0	8.0/14.6/3.3 8.6 ± 5.7	7.8/14.0/3.0 8.3 ± 5.5
T2c	48.2/54.5/49.3 50.7 ± 3.4	41.7/48.2/43.3 44.4 ± 3.4	14.9/25.9/18.9 19.9 ± 5.6	2.3/8.1/5.7 5.3 ± 2.9	1.3/6.3/4.2 3.9 ± 2.5	0.9/2.4/1.8 1.7 ± 0.7
T3c	33.2/39.0/42.6 38.3 ± 4.8	10.0/29.4/24.6 21.3 ± 10.1	2.8/17.0/12.8 10.9 ± 7.3	0.5/3.5/2.6 2.2 ± 1.5	0.2/0.6/0.5 0.4 ± 0.2	0.2/0.1/0.2 0.2 ± 0.0

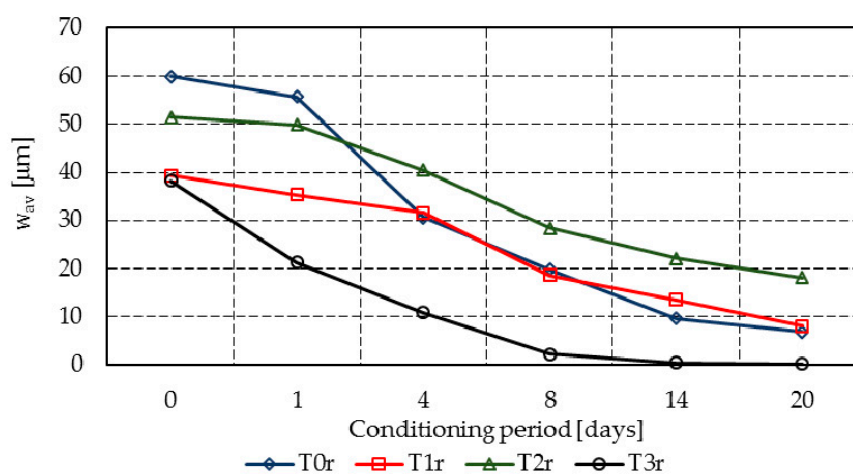


Figure 4. Mean crack progress in mixtures T0r–T3r.

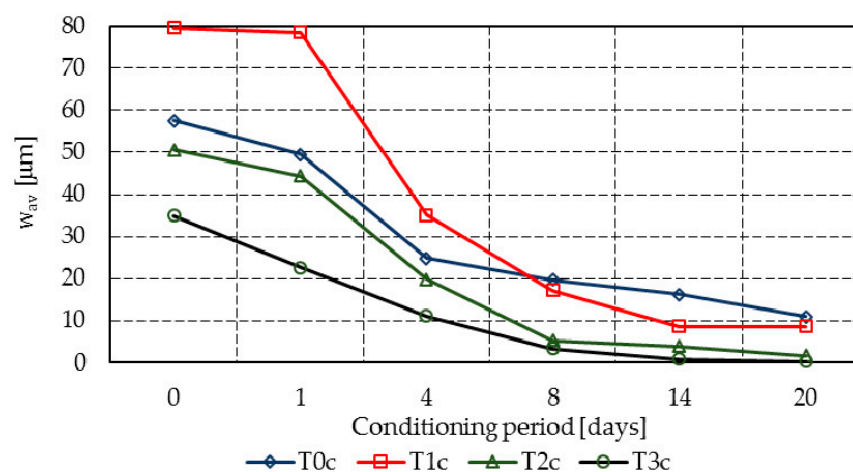


Figure 5. Mean crack progress in mixtures T0c–T3c.

Despite the initial predictions, the maximum aggregate size was not found to influence the initial cracking behavior. While mixture T0r registered a crack width similar to T0c (i.e., just 2.4 μm larger), the same tendency was also found in the rest of the mixes, except mixes T1r and T1c, where the results are significantly different.

Mixtures T3r and T3c entirely or almost entirely filled the cracks within 14 days, at which point the registered closure rates were 98.9% and 97.3%, respectively. However, at 20 days, T3r reached 99.6% and T3c reached 99.3%, while the reference mixes T0r and T0c presented closure rates of 88.6% and 80.8%, respectively (see Figure 6 compared to Figure 7).

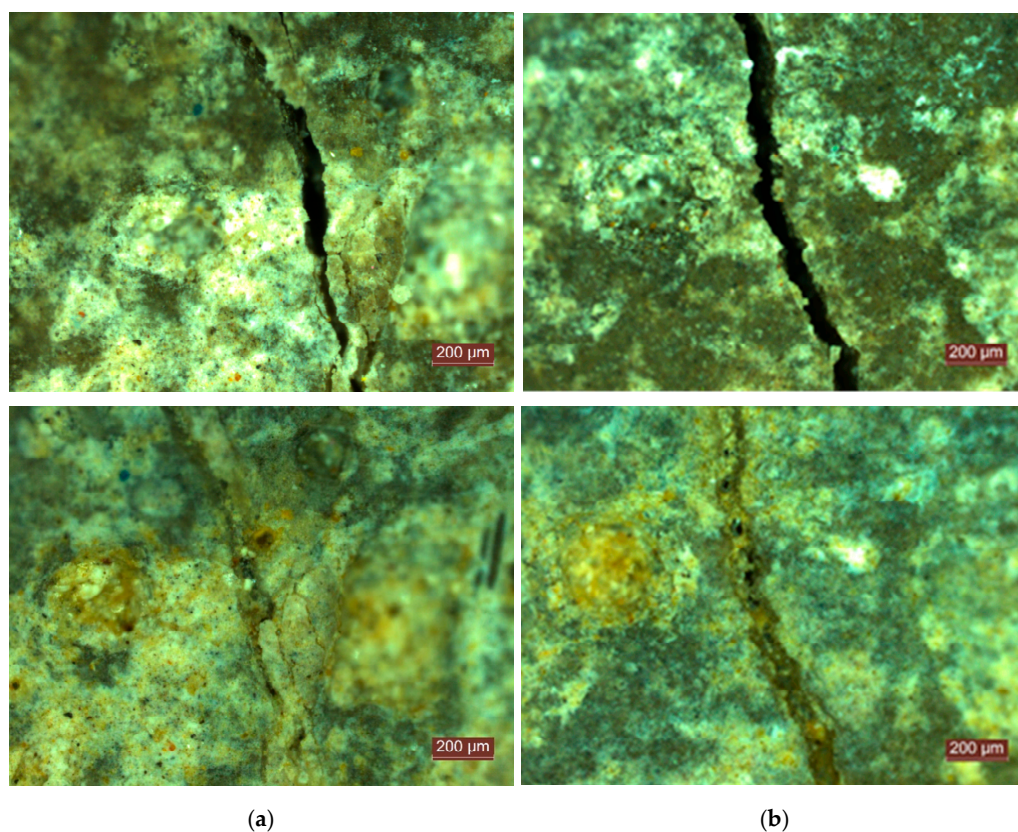


Figure 6. Initial crack and self-sealing products at 20 days of the reference mixes: (a) T0r; (b) T0c.

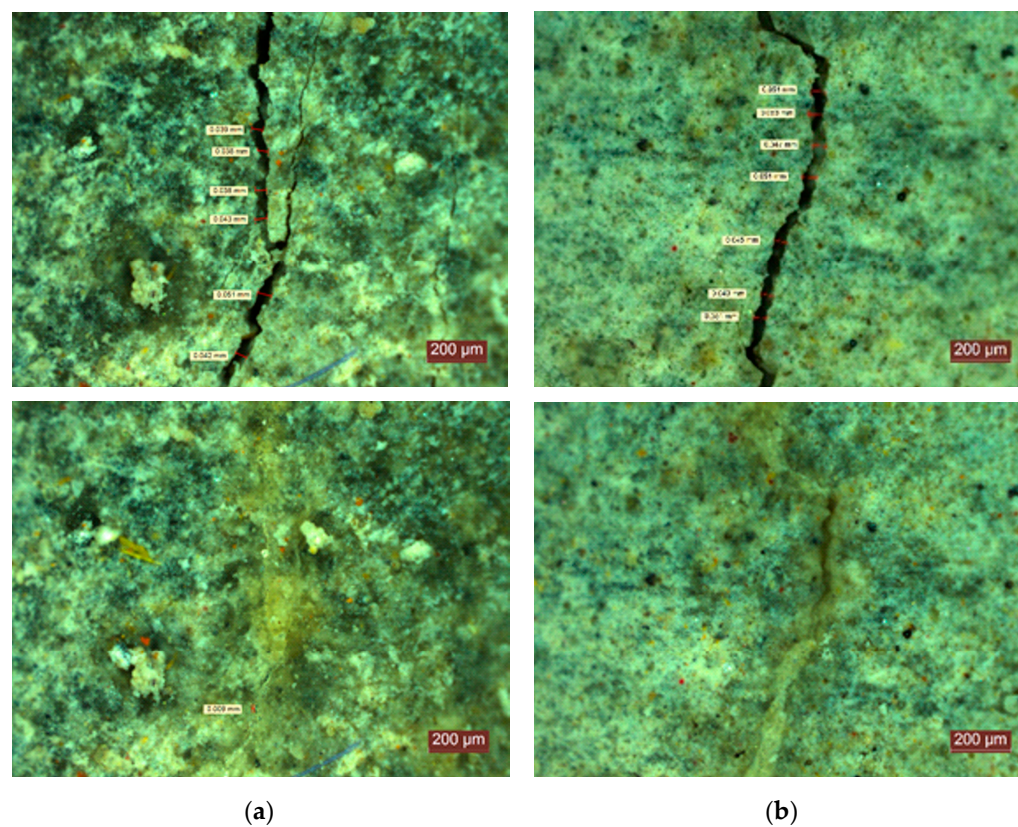


Figure 7. Initial crack and self-sealing products at 20 days for an ICW content of 3%: (a) T3r; (b) T3c.

Mixture T2c achieved a similar performance, with a crack closure of 96.7% at 20 days. Mixtures T1c and T1r had similar tendencies (i.e., crack closures of 79.5% and 89.2%, respectively, at 20 days), while the results for T2r were divergent (i.e., just 64.7% at 20 days).

Figure 8 presents the raw segmented data for the crack closure and Figure 9 shows the Gaussian distribution registered for the raw segmented data. Considering the physical significance of the crack closure is described as a value between 0% and 100%, Table 5 presents the mean crack closure and standard deviation at 20 days, and the probabilities of reaching several different intervals of crack closure. In probabilistic terms, the 3% ICW powder showed the best sealing capacity for both mixture types. At 20 days, T3r showed a probability of 0.36 of full closure, and a probability of 0.98 of at least 75% closure, while T3c had a full closure probability of 0.35, and a probability of 0.98 for a closure of more than 75%. A mention should be made of the reduction in the standard deviation, which dropped spectacularly at 20 days with the ICW content of 3%. T2c, with an ICW content of 2%, presented a similar closure trend.

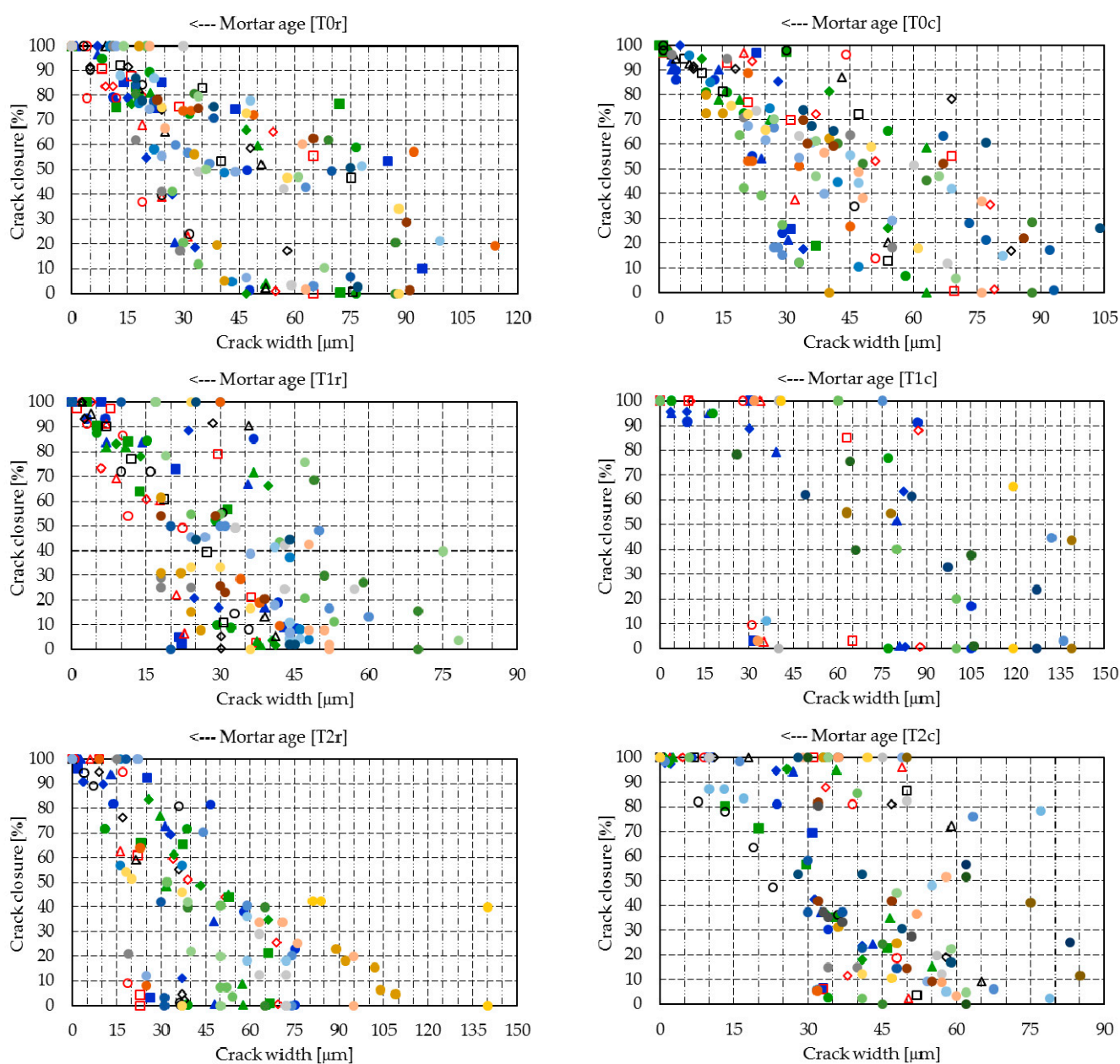


Figure 8. Cont.

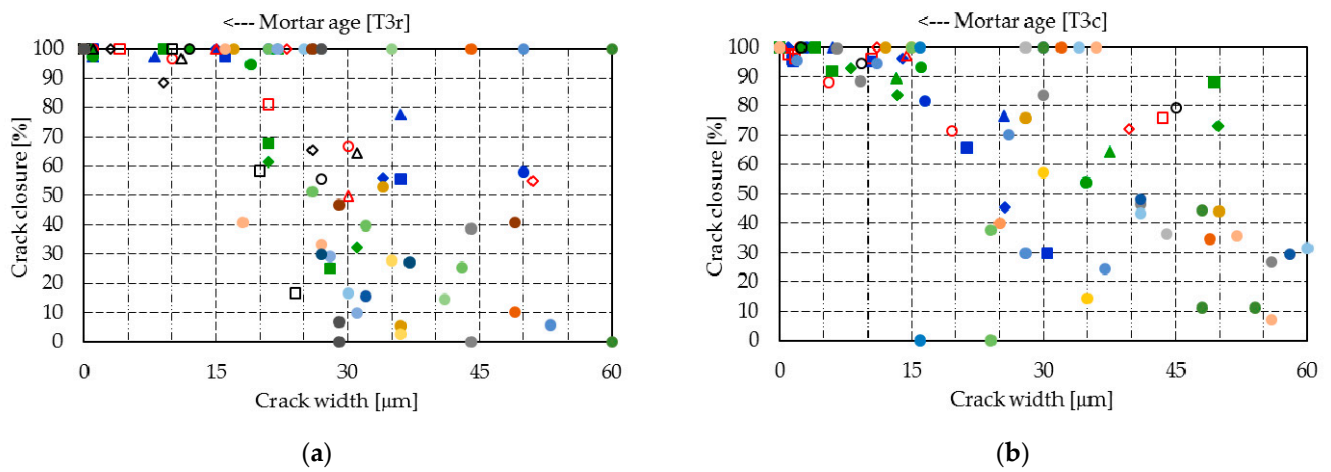


Figure 8. Segmented crack closures—markers correspond to the readings of each crack segment: (a) T0r–T3r; (b) T0c–T3c.

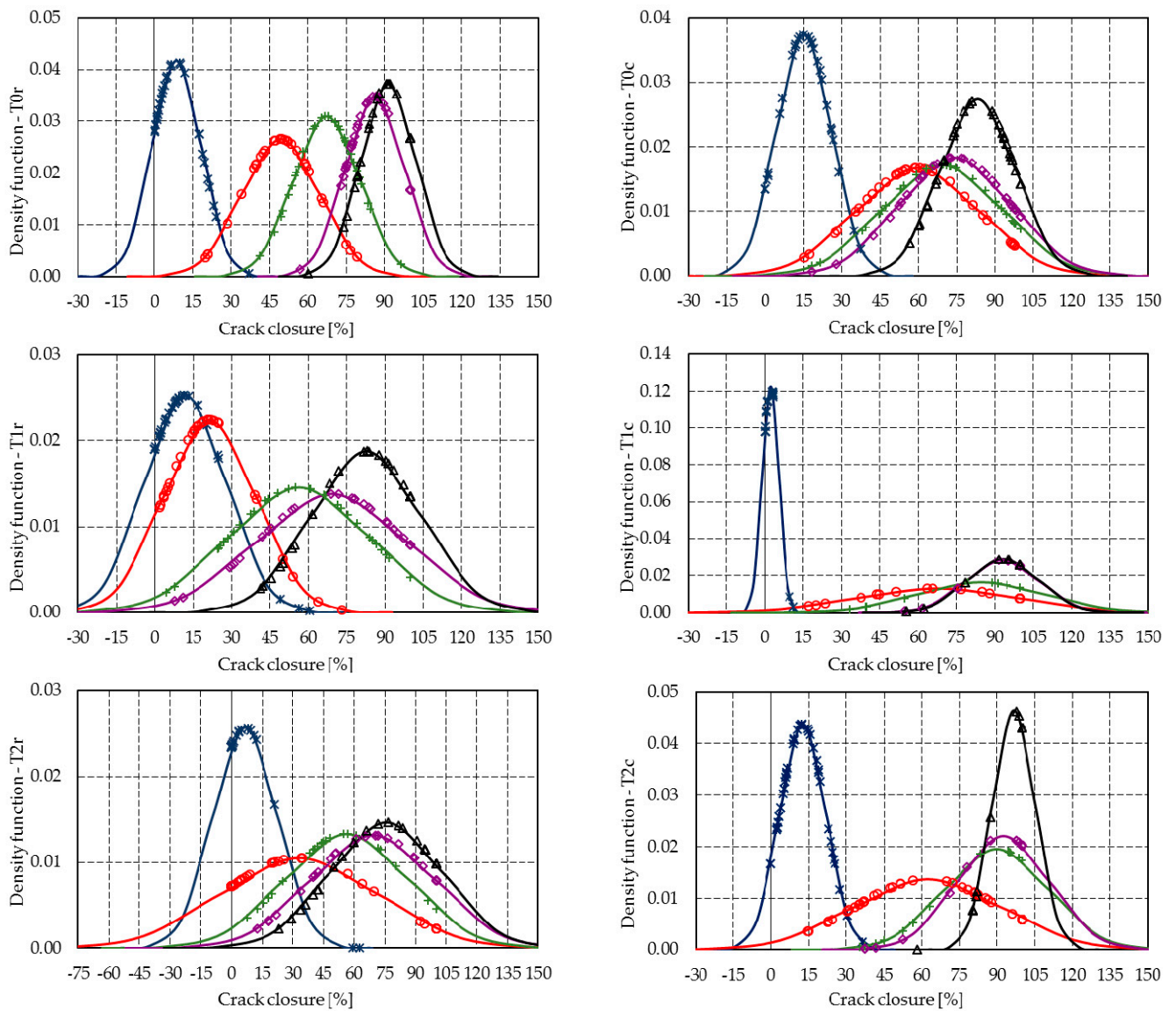


Figure 9. Cont.

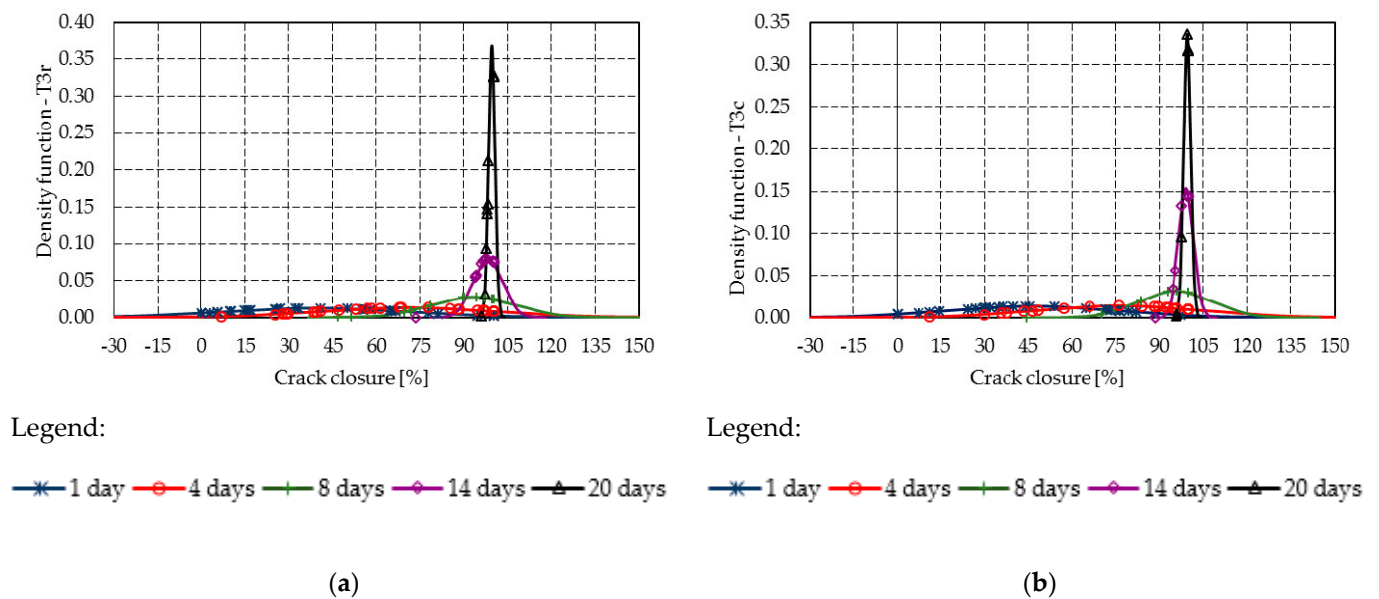
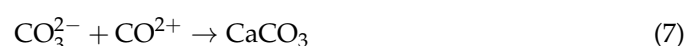


Figure 9. Gaussian distributions of the crack closure: (a) T0r–T3r; (b) T0c–T3c.

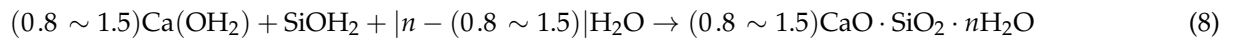
Table 5. Probabilistic parameters and probabilities of crack closure at 20 days.

Mixture	μ/σ (%)	Probabilities for Significant Crack Closure Intervals of		
		$\geq 50\%$ and $< 75\%$	$\geq 75\%$ and $< 100\%$	100%
T0r	91.3/10.7	0.07	0.59	0.21
T1r	82.7/21.2	0.20	0.43	0.21
T2r	75.7/27.2	0.33	0.32	0.19
T3r	99.5/1.0	0.00	0.62	0.36
T0c	83.4/14.6	0.17	0.69	0.13
T1c	93.2/13.7	0.15	0.53	0.31
T2c	96.7/8.6	0.02	0.64	0.35
T3c	96.7/10.7	0.00	0.63	0.35

The results clearly show that, in structural mortars made with Portland cement and fly ash in similar proportions, ICW contributes to the sealing of crack widths of up to 100 μm within 20 days. Sisomphon et al. [22] reported the sealing of cracks up to 400 μm at 28 days in mortars made with Portland cement. Research performed by Roig-Flores et al. [41] and Ferrara et al. [39] confirms these results. Jaroenratanapirom and Sahamitmongkol [53] investigated mortars containing various additional cementitious materials, such as fly ash. They concluded that all mortars show a self-healing capacity to some extent. For crack widths up to 50 μm , ICW showed the best self-healing capacity. Chandra et al. [54] found that a 30% fly ash content and a 1.5% ICW content achieve 102% mechanical strength recovery under water immersion conditions. After water immersion, wet–dry cycles ensure the best self-healing performance. Wang et al. [55] concluded recently that the excessive use of fly ash has a negative impact upon the mortar’s self-healing potential if the content is over 10 wt. %. However, the contributions of both fly ash and ICW are considerably increased by the presence of water. When ICW is added to cementitious materials, the main healing product is CaCO_3 . The sealing closure is related to the concentration of Ca^{2+} , CO_2 , and water at the crack entrance. The chemical reactions are:



Even if the fly ash content does not affect the crystallization reaction of ICW, it generates C–S–H gel and helps with crack self-sealing via the reaction:



3.2. Self-Sealing Closure Rate

Figures 10 and 11 summarize the crack closure rate of the individual cracks, Figure 12 presents the raw segmented data for the crack closure, and Figure 13 shows the Gaussian distributions of the closure rate.

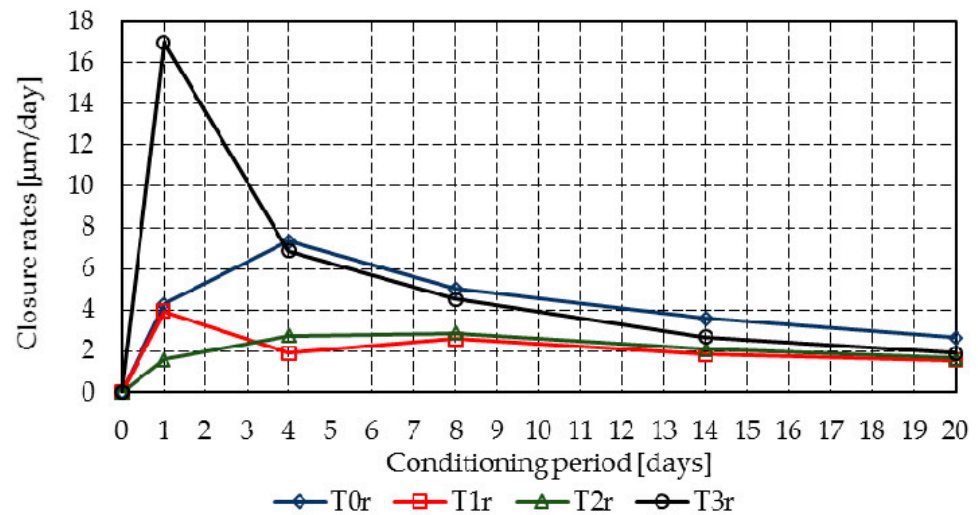


Figure 10. Mean closure rates in mixtures T0r-T3r.

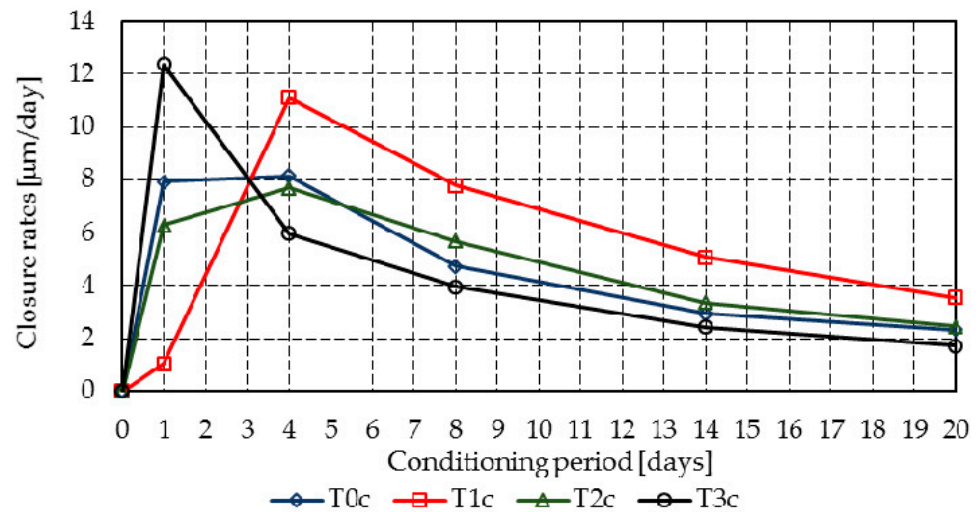


Figure 11. Mean closure rates in mixtures T0c-T3c.

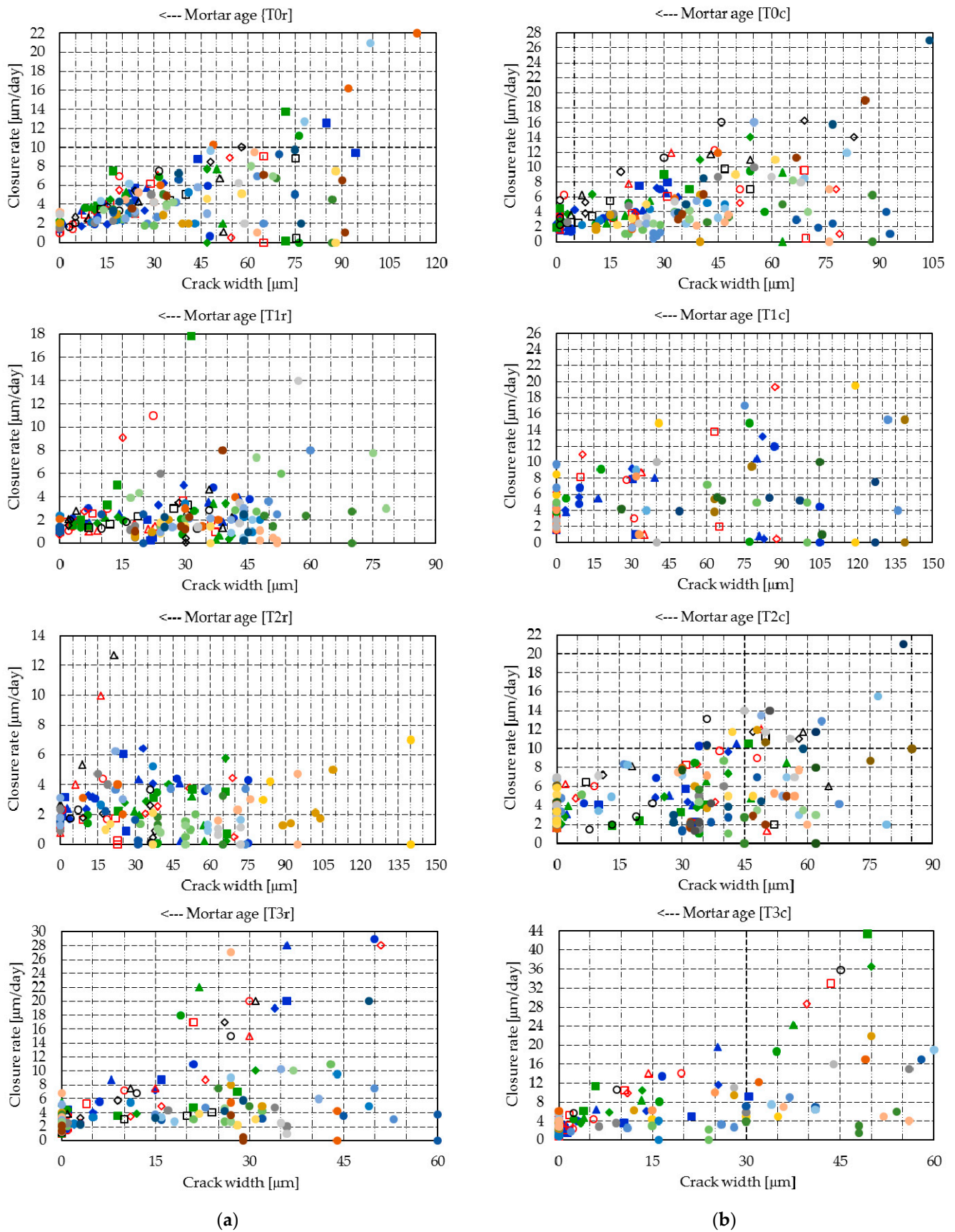
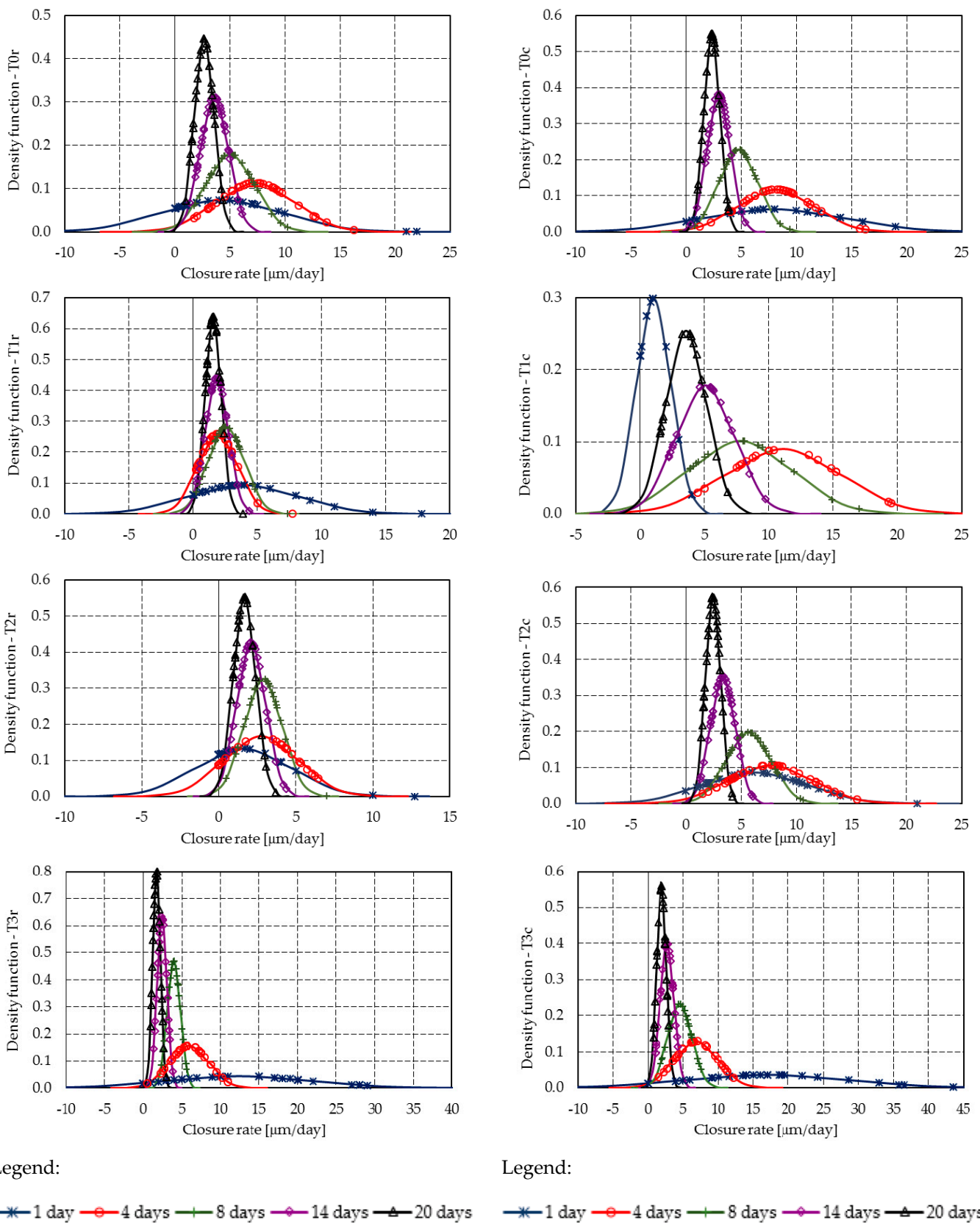


Figure 12. Segmented closure rates—markers correspond to the readings of each crack segment: (a) T0r–T3r; (b) T0c–T3c.



(a) (b)
 Figure 13. Gaussian distributions of the closure rate: (a) T0r–T3r; (b) T0c–T3c.

Mixtures T3r and T3c achieved a high initial closure rate of 12.4 $\mu\text{m}/\text{day}$ and 17.0 $\mu\text{m}/\text{day}$, all other mixtures having closure rates below 8.0 $\mu\text{m}/\text{day}$, with the exception of mixture T1c, which reached 11.1 $\mu\text{m}/\text{day}$ on the fourth day. All mixtures presented a gradual reduction in the mean closure rate up to 20 days. However, due to the delayed hydration of fly ash, further increases may occur.

Because the results of the probabilistic analysis are strongly influenced by the closure of many crack segments, the analysis will be made on mortar at 8 days of age. Table 6 shows the probabilistic parameters and the probabilities of various significant closure rates at 8 days.

Table 6. Probabilistic parameters and probabilities of closure rates at 8 days.

Mixture	μ/σ [%]	Probability of Closure Rates		
		$\geq 1 \mu\text{m}/\text{day}$	$\geq 3 \mu\text{m}/\text{day}$	$\geq 6.0 \mu\text{m}/\text{day}$
T0r	5.02/2.22	0.97	0.78	0.35
T1r	1.56/0.63	0.87	0.38	0.01
T2r	2.88/1.22	0.94	0.45	0.01
T3r	3.95/0.50	0.99	0.87	0.01
T0c	4.73/1.74	1.00	0.78	0.26
T1c	7.78/3.94	0.96	0.89	0.68
T2c	5.67/2.02	1.00	0.91	0.42
T3c	1.91/0.71	1.00	0.81	0.19

At 8 days, despite the fact that mixtures T1c and T2c display the highest likelihood of achieving closure rates above 6 $\mu\text{m}/\text{day}$ (i.e., at least 120 μm crack closure in 20 days), for closure rates above 3 $\mu\text{m}/\text{day}$ (i.e., at least 60 μm crack closure in 20 days), mixes T0r and T0c–T3c achieve similar probabilities, which vary between 0.78 and 0.91. It must be noted that, within 1 day, T3r and T3c developed the highest closure rates.

4. Conclusions

Here, the influence of ICW content (i.e., 1–3% of Portland cement mass) upon early-age crack sealing in structural mortar has been investigated. The experimental evidence clearly shows that an ICW content of 3% achieves the best crack closure ability. However, these values are also influenced by the mechanical properties that govern the initial crack's width, the fracturing mode, and most importantly, the exposure conditions. In probabilistic terms, all the analyzed mixtures showed a significant ability to fill cracks with widths of up to 90–180 μm at early ages of up to a month.

The autogenous early-age self-sealing potential displayed by mortar mixtures with a maximum grain size below 4 mm is clear, and opens the way for larger well-graded aggregates with adequate self-sealing/self-healing abilities, which can also achieve superior time-dependent mechanical performances.

Author Contributions: Conceptualization, T.-P.T. and C.M.; methodology, T.-P.T. and C.M.; validation, A.H., A.M., C.M. and B.-A.I.; formal analysis, T.-P.T., C.M. and B.-A.I.; investigation, T.-P.T. and C.M.; resources, A.H.; data curation, T.-P.T. and C.M.; writing—original draft preparation, C.M. and T.-P.T.; writing—review and editing, C.M. and A.M.; supervision, C.M.; project administration, T.-P.T.; funding acquisition, A.H. and A.M. All authors have read and agreed to the published version of the manuscript.

Funding: This research was financially supported by the Project “Entrepreneurial competences and excellence research in doctoral and postdoctoral programs-ANTREDOC”, project co-funded by the European Social Fund financing agreement no. 56437/24.07.2019.

Institutional Review Board Statement: Not applicable.

Informed Consent Statement: Not applicable.

Data Availability Statement: The data presented in this study are available on request from the authors.

Acknowledgments: The authors would like to thank Michael Grantham of Sandberg LLP (former Visiting Professor at The University of Leeds and Queen’s University Belfast, and Past President of the Institute of Concrete Technology, UK) for his support and contribution in technical editing, language editing and proofreading.

Conflicts of Interest: The authors declare no conflict of interest.

References

- Lauer, K.R.; Slate, F.O. Autogenous healing of cement paste. *J. Am. Concr. Inst.* **1956**, *52*, 1083–1097. [[CrossRef](#)]
- Hearn, N.; Morley, C.T. Self-sealing property of concrete—Experimental evidence. *Mater. Struct.* **1997**, *30*, 404–411. [[CrossRef](#)]
- Hyde, G.W.; Smith, W.J. Results of experiments made to determine the permeability of cements and cement mortars. *J. Frankl. Inst. Phila.* **1889**, *128*, 199–207. [[CrossRef](#)]
- Glanville, W.H. The permeability of Portland cement concrete. *Build. Res. J.* **1931**, *3*, 1–61.
- Ruttgers, A.; Vidal, E.N.; Wing, S.P. An investigation of the permeability of mass concrete with particular reference to Boulder Dam. *J. Am. Concr. Inst.* **1935**, *6*, 389–416.
- Bissonnette, B.; Pigeon, M. Tensile creep at early ages of ordinary, silica fume and fiber reinforced concretes. *Cem. Concr. Res.* **1995**, *25*, 1075–1085. [[CrossRef](#)]
- Altoubat, S.; Lange, D.A. Creep, Shrinkage and Cracking of Restrained Concrete at Early Age. *ACI Mater. J.* **2001**, *98*, 323–331.
- Mircea, C.; Filip, M.; Ioani, A. Investigation of Cracking of Mass Concrete Members Induced by Restrained Contraction, SP-246: Structural Implications of Shrinkage and Creep of Concrete. In Proceedings of the ACI Convention, Fajardo, Puerto Rico, 14–18 October 2007; Gardner, J., Chiorino, M.A., Eds.; ACI: Farmington Hills, MI, USA, 2007; Volume SP-246-14, pp. 229–246.
- Edvardsen, C. Water permeability and autogenous healing of cracks in concrete. *ACI Mater. J.* **1999**, *96*, 448–454.
- Li, M.; Li, V.C. Cracking and healing of engineered cementitious composites under chloride environment. *ACI Mater. J.* **2011**, *108*, 333–340.
- Mihashi, H.; Nishiwaki, T. Development of Engineered Self-Healing and Self-Repairing Concrete- State-of-the-Art Report. *J. Adv. Concr. Technol.* **2012**, *10*, 170–184. [[CrossRef](#)]
- Van Tittelboom, K.; De Belie, N. A Self-Healing in Cementitious Materials—A Review. *Materials* **2013**, *6*, 2182–2217. [[CrossRef](#)] [[PubMed](#)]
- Herbert, E.N.; Li, V.C. Self-Healing of Microcracks in Engineered Cementitious Composites (ECC) under a Natural Environment. *Materials* **2013**, *6*, 2831–2845. [[CrossRef](#)] [[PubMed](#)]
- De Belie, N.; Gruyaert, E.; Al-Tabbaa, A.; Antonaci, P.; Baera, C.; Bajare, D.; Darquennes, A.; Davies, R.; Ferrara, L.; Jefferson, T.; et al. A Review of Self-Healing Concrete for Damage Management of Structures. *Adv. Mater. Interfaces* **2018**, *5*, 1800074. [[CrossRef](#)]
- Danish, A.; Mosaberpanah, M.A.; Salim, M.U. Past and present techniques of self-healing in cementitious materials: A critical review on efficiency of implemented treatments. *J. Mater. Res. Technol.* **2020**, *9*, 6883–6899. [[CrossRef](#)]
- Fernandez, C.A.; Correa, M.; Nguyen, M.T.; Rod, K.A.; Dai, G.L.; Cosimbescu, L.; Rousseau, R.; Glezakou, V.A. Progress and challenges in self-healing cementitious materials. *J. Mater. Sci.* **2021**, *56*, 201–230. [[CrossRef](#)]
- Yang, Y.; Lepech, M.D.; Yang, E.H.; Li, V.C. Autogenous healing of engineered cementitious composites under wet-dry cycles. *Cem. Concr. Res.* **2009**, *39*, 382–390. [[CrossRef](#)]
- Van Tittelboom, K.; Gruyaert, E.; Rahier, H.; De Belie, N. Influence of mix composition on the extent of autogenous crack healing by continued hydration or calcium carbonate formation. *Constr. Build. Mater.* **2012**, *37*, 349–359. [[CrossRef](#)]
- Snoeck, D.; De Belie, N. From straw in bricks to modern use of microfibres in cementitious composites for improved autogenous healing—A review. *Constr. Build. Mater.* **2015**, *95*, 774–787. [[CrossRef](#)]
- Snoeck, D.; De Belie, N. Autogenous healing in strain-hardening cementitious materials with and without superabsorbent polymers: An 8-year study. *Front. Mater.* **2019**, *6*, 1–12. [[CrossRef](#)]
- Neville, A. Autogenous healing—A concrete miracle? *Concr. Int.* **2002**, *24*, 76–82.
- Sisomphon, K.; Copuroglu, O.; Koenders, E.A.B. Self-healing of surface cracks in mortars with expansive additive and crystalline additive. *Cem. Concr. Compos.* **2012**, *34*, 566–574. [[CrossRef](#)]
- Hilloulin, B.; Hilloulin, D.; Grondin, F.; Loukili, A.; De Belie, N. Mechanical regains due to self-healing in cementitious materials: Experimental measurements and micro-mechanical model. *Cem. Concr. Res.* **2016**, *80*, 21–32. [[CrossRef](#)]
- Ferrara, L.; Krelani, V.; Morreti, F. Autogenous healing on the recovery of mechanical performance of High Performance Fibre Reinforced Cementitious Composites (HPFRCCs): Part 2—Correlation between healing of mechanical performance and crack sealing. *Cem. Concr. Compos.* **2016**, *73*, 299–315. [[CrossRef](#)]
- Lăzărescu, A.; Szilagy, H.; Ioani, A.; Baeră, C. Parameters Affecting the Mechanical Properties of Fly Ash-Based Geopolymer Binders—Experimental Results. *IOP Conf. Ser. Mater. Sci. Eng.* **2018**, *374*, 012035. [[CrossRef](#)]
- Voinitchi, C.; Baeră, C.; Zapciu, M.; Matei, C.; Szilagy, H. Development of Cement-Based Materials Enriched with Polymeric Coated Reactive Grains as Long-Term Promoter of Matrix Continuous Hydration. *IOP Conf. Ser. Mater. Sci. Eng.* **2020**, *877*, 012028. [[CrossRef](#)]
- Szilagy, H.; Baeră, C.; Lăzărescu, A.; Mircea, A.C. Preliminary evaluation of local mineral additions (by-products or wastes) valorisation in innovative cementitious composites. *Constructions* **2018**, *19*, 3–10.

28. Huang, H.; Ye, G.; Damidot, D. Effect of blast furnace slag on self-healing of microcracks in cementitious materials. *Cem. Concr. Res.* **2014**, *60*, 68–82. [[CrossRef](#)]
29. Olivier, K.; Darquennes, A.; Benboudj, F.; Gagné, R. Early-Age Self-Healing of Cementitious Materials Containing Ground Granulated Blast-Furnace Slag under Water Curing. *J. Adv. Concr. Technol.* **2016**, *14*, 717–727. [[CrossRef](#)]
30. Zhang, Z.; Qian, S.; Ma, H. Investigating mechanical properties and self-healing behavior of micro-cracked ECC with different volume of fly ash. *Constr. Build. Mater.* **2014**, *52*, 17–23. [[CrossRef](#)]
31. Yildirim, G.; Sahmaran, M.; Ahmed, H.U. Influence of Hydrated Lime Addition on the Self-Healing Capability of High-Volume Fly Ash Incorporated Cementitious Composites. *J. Mater. Civ. Eng.* **2015**, *27*, 4014187. [[CrossRef](#)]
32. Siad, H.; Alyousif, A.; Keskin, O.K.; Keskin, S.B.; Lachemi, M.; Sahmaran, M.; Hossain, K.M.A. Influence of limestone powder on mechanical, physical and self-healing behavior of Engineered Cementitious Composites. *Constr. Build. Mater.* **2015**, *99*, 1–10. [[CrossRef](#)]
33. Ouyang, W.; Koleva, D.A.; Ye, G.; Van Breugel, K. Insights into the mechanisms of nucleation and growth of C–S–H on fillers. *Mater. Struct.* **2017**, *50*, 213. [[CrossRef](#)]
34. Scrivener, K.; Ouzia, A.; Juillard, P.; Mohamed, A.K. Advances in understanding cement hydration mechanisms. *Cem. Concr. Res.* **2019**, *124*, 105823. [[CrossRef](#)]
35. Bacarji, E.; Toledo Filho, R.D.; Koenders, E.A.B.; Figueiredo, E.P.; Lopes, J.L.M.P. Sustainability perspective of marble and granite residues as concrete fillers. *Cem. Concr. Compos.* **2013**, *45*, 1–10. [[CrossRef](#)]
36. Snoeck, D.; De Belie, N. Repeated Autogenous Healing in Strain-Hardening Cementitious Composites by Using Superabsorbent Polymers. *J. Mater. Civ. Eng.* **2013**, *25*, 864–870.
37. Huang, X.; Ge, J.; Kaewunruen, S.; Su, Q. The Self-Sealing Capacity of Environmentally Friendly, Highly Damped, Fibre-Reinforced Concrete. *Materials* **2020**, *13*, 298. [[CrossRef](#)] [[PubMed](#)]
38. Li, Z.; Wyrzykowski, M.; Dong, H.; Granja, H.; Azenha, M.; Lura, P.; Ye, G. Internal curing by superabsorbent polymers in alkali-activated slag. *Cem. Concr. Res.* **2020**, *135*, 106123. [[CrossRef](#)]
39. Ferrara, L.; Cuenca, E.; Tejedor, A.; Brac, E.G. Performance of concrete with and without crystalline admixtures under repeated cracking/healing cycles. In Proceedings of the International Conference on Concrete Repair, Rehabilitation and Retrofitting, Cape Town, South Africa, 19–21 November 2018; Alexander, M.G., Dehn, F., Moyo, P., Eds.; EDP Sciences: Les Ulis, France, 2018; Volume 199, pp. 1–6.
40. Roig-Flores, M.; Moscato, S.; Serna, P.; Ferrara, L. Self-healing capability of concrete with crystalline admixtures in different environments. *Constr. Build. Mater.* **2015**, *86*, 1–11. [[CrossRef](#)]
41. Roig-Flores, M.; Pirritano, F.; Serna, P.; Ferrara, L. Effect of crystalline admixtures on the self-healing capability of early-age concrete studied by means of permeability and crack closing tests. *Constr. Build. Mater.* **2016**, *114*, 447–457. [[CrossRef](#)]
42. Buller, A.S.; Abro, F.R.; Lee, K.M.; Jamg, S.Y. Mechanical Recovery of Cracked Fiber-Reinforced Mortar Incorporating Crystalline Admixture, Expansive Agent, and Geomaterial. *Adv. Mater. Sci. Eng.* **2019**, *2019*, 3420349. [[CrossRef](#)]
43. Park, B.; Choi, Y.C. Self-healing capability of cementitious materials with crystalline admixtures and super absorbent polymers (SAPs). *Constr. Build. Mater.* **2018**, *189*, 1054–1066. [[CrossRef](#)]
44. Azarsa, P.; Gupta, R.; Biparva, A. Assessment of self-healing and durability parameters of concretes incorporating crystalline admixtures and Portland Limestone Cement. *Cem. Concr. Compos.* **2019**, *99*, 17–23. [[CrossRef](#)]
45. Li, D.; Chen, B.; Chen, X.; Fu, B.; Wei, H.; Xiang, X. Synergetic effect of superabsorbent polymer (SAP) and crystalline admixture (CA) on mortar macro-crack healing. *Constr. Build. Mater.* **2020**, *247*, 118521. [[CrossRef](#)]
46. Rhee, I.; Lee, J.S.; Roh, Y.S. Fracture Parameters of Cement Mortar with Different Structural Dimensions under the Direct Tension Test. *Materials* **2019**, *12*, 1850. [[CrossRef](#)] [[PubMed](#)]
47. Elices, M.; Rocco, C.G. Effect of aggregate size on the fracture and mechanical properties of a simple concrete. *Eng. Fract. Mech.* **2008**, *75*, 3839–3851. [[CrossRef](#)]
48. Karamloo, M.; Mazloom, M.; Payganeh, G. Effects of maximum aggregate size on fracture behaviors of self-compacting lightweight concrete. *Constr. Build. Mater.* **2016**, *123*, 508–515. [[CrossRef](#)]
49. Mircea, A.C.; Toader, T.P. Designing Concrete with Self-healing Properties Using Engineered Cementitious Composites as a Model. *IOP Conf. Ser. Mater. Sci. Eng.* **2020**, *877*, 012035. [[CrossRef](#)]
50. Nishiwaki, T.; Koda, M.; Yamada, M.; Mihashi, H.; Kikuta, T. Experimental Study on Self-Healing Capability of FRCC Using Sifferent Types of Synthetic Fibers. *J. Adv. Concr. Technol.* **2012**, *10*, 195–206. [[CrossRef](#)]
51. Henseler, J.; Ringle, C.; Sinkovics, R. The use of partial least squares path modeling in international marketing. *Adv. Int. Mark.* **2009**, *20*, 277–320.
52. Cuenca, E.; Rigamonti, E.; Brac, E.G.; Ferrara, L.B. Crystalline Admixture as Healing Promoter in Concrete Exposed to Chloride-Rich Environments: Experimental Study. *J. Mater. Civ. Eng.* **2021**, *33*, 04020491. [[CrossRef](#)]
53. Jaroenratanapirom, D.; Sahamitmongkol, R. Effects of Different Mineral Additives and Cracking Ages on Self-healing Performance of Mortar. In Proceedings of the 6th Annual Concrete Conference, Phetchaburi, Thailand, 20–23 October 2010.
54. Wang, X.; Qiao, H.; Zhang, Z.; Tang, S.; Liu, S.; Niu, M.; Li, G. Effect of fly ash on the self-healing capability of cementitious materials with crystalline admixture under different conditions. *AIP Adv.* **2021**, *11*, 075018. [[CrossRef](#)]
55. Reddy, T.C.S.; Ravitheja, A.; Sashidhar, C. Self-Healing Ability of High-Strength Fibre-Reinforced Concrete with Fly Ash and Crystalline Admixture. *Civ. Eng. J.* **2018**, *4*, 971–979. [[CrossRef](#)]